Bacterial Cytosine Deaminase Mutants Created by Molecular Engineering Show Improved 5-Fluorocytosine–Mediated Cell Killing *In vitro* and *In vivo*

Michi Fuchita,[1] Andressa Ardiani,[1] Lei Zhao,[3] Kinta Serve,[1] Barry L. Stoddard,[3] and Margaret E. Black[1,2]

[1]School of Molecular Biosciences and [2]Department of Pharmaceutical Sciences, Washington State University, Pullman, Washington; and [3]Fred Hutchinson Cancer Research Center and the Graduate Program in Molecular and Cell Biology, University of Washington, Seattle, Washington

Abstract

Cytosine deaminase is used in combination with 5-fluorocytosine as an enzyme-prodrug combination for targeted genetic cancer treatment. This approach is limited by inefficient gene delivery and poor prodrug conversion activities. Previously, we reported individual point mutations within the substrate binding pocket of bacterial cytosine deaminase (bCD) that result in marginal improvements in the ability to sensitize cells to 5-fluorocytosine (5FC). Here, we describe an expanded random mutagenesis and selection experiment that yielded enzyme variants, which provide significant improvement in prodrug sensitization. Three of these mutants were evaluated using enzyme kinetic analyses and then assayed in three cancer cell lines for 5FC sensitization, bystander effects, and formation of 5-fluorouracil metabolites. All variants displayed 18- to 19-fold shifts in substrate preference toward 5FC, a significant reduction in IC_{50} values and improved bystander effect compared with wild-type bCD. In a xenograft tumor model, the best enzyme mutant was shown to prevent tumor growth at much lower doses of 5FC than is observed when tumor cells express wild-type bCD. Crystallographic analyses of this construct show the basis for improved activity toward 5FC, and also how two different mutagenesis strategies yield closely related but mutually exclusive mutations that each result in a significant alteration of enzyme specificity. [Cancer Res 2009;69(11):4791–9]

Introduction

Cytosine deaminase (CD; EC 3.5.4.1) is responsible for the conversion of cytosine to uracil and ammonia, providing an important mechanism for pyrimidine salvage in microbes. Because this activity is not found in mammalian cells (1, 2), CD is being explored for use in suicide gene therapy (SGT) due to its ability to also convert the antifungal agent 5-fluorocytosine (5FC) to the potent antimetabolite, 5-fluorouracil (5FU; refs. 3–6). Intracellularly, 5FU is subsequently metabolized by endogenous enzymes to 5FdUMP, an irreversible inhibitor of thymidylate synthetase, thereby restricting the production of dTMP and downstream phosphorylated products. Depletion of dTTP pools results in inhibition of DNA synthesis and leads to apoptosis (7–9). A phenomenon known as the bystander effect provides an extension of cell killing beyond the cells expressing the suicide gene to neighboring cells (10–13). A combination of factors is thought to participate in the bystander effect including transfer of antimetabolites and/or suicide enzymes through gap junctions, diffusion, and apoptotic vesicles. An immune-related response also contributes to the bystander effect, although in a delayed fashion. A potent bystander effect is critical to successful tumor ablation especially in light of the inefficient viral and nonviral gene delivery systems currently available. To support an effective bystander effect, sufficient antimetabolites must be generated in suicide enzyme-expressing cells.

Unfortunately, wild-type CD displays relatively poor turnover of 5FC, thus limiting the overall therapeutic response. As such, high doses of 5FC are necessary and result in undesirable side effects primarily due the presence of microbes in the intestinal tract that encode CD. The rapid half-life of 5FC in blood serves to further limit the availability of 5FC at the tumor site. To overcome the constraints associated with poor 5FC activation, we sought to optimize the activity of bacterial cytosine deaminase (bCD) toward 5FC using regio-specific random mutagenesis by targeting two key regions of the active site. From earlier studies, residue D314 in wild-type bCD was shown to play a key role in substrate recognition (14, 15). In particular, the D314G and D314S substitutions display a shift in substrate preference toward 5FC. However, these variants provide only a modest 2- to 4-fold decrease in IC_{50} for 5FC *in vitro* compared with wild-type bCD–expressing tumor cells.

Using structural information as well as previous mutagenesis results, two regions lining the active site of bCD (residues 149–159 and 310–320; Fig. 1) were targeted for random mutagenesis to identify mutants with further enhanced 5FC sensitivity *in vitro* and *in vivo* (16, 17). Such optimized CD variants that allow lower, less toxic 5FC doses to achieve efficient cell killing and an enhanced bystander effect will likely provide meaningful and significant clinical benefit when used in SGT protocols for the treatment of a variety of cancers.

Materials and Methods

Materials. Oligonucleotides were obtained from IDT. Enzymes were purchased from New England Biolabs. Polyclonal bCD-antibody was generated by Harlan. DNA purification was done using Wizard-PCR kit, HiSpeed-Plasmid Mini kit (Qiagen), and StrataPrep EF-Plasmid Midikit (Stratagene). Alamar Blue was purchased from Serotec. Nickel affinity chromatography reagents were purchased from Qiagen. All cell culture reagents were purchased from Life Technologies. All other reagents were purchased from Sigma unless otherwise noted.

Note: Supplementary data for this article are available at Cancer Research Online (http://cancerres.aacrjournals.org/).

M. Fuchita and A. Ardiani are joint first authors.

Requests for reprints: Margaret E. Black, Department of Pharmaceutical Sciences, P. O. Box 646534, Washington State University, Pullman, WA 99164-6534. Phone: 509-335-6265; Fax: 509-335-5902; E-mail: blackm@mail.wsu.edu.

doi:10.1158/0008-5472.CAN-09-0615

Bacterial strains. *Escherichia coli* strain GIA39, which is deficient in CD and orotidine 5′-phosphate decarboxylase activities, was used in the genetic complementation assays for CD activity (15). The *E. coli* strains NM522 and XL1-Blue were used as recipients for certain cloning and mutagenesis procedures. *E. coli* BL21 (DE3) and BL21-RIL (Novagen) were used for protein purification.

Cell lines. Rat C6 glioma cells (C6) were purchased from American Type Culture Collection (ATCC). Human colorectal carcinoma cells (HCT116) and human prostate carcinoma cells (DU145) were provided by Dr. Neal Davies (Washington State University, Pullman, WA). Growth conditions for the cell lines are described in detail by ATCC. Transfected cells were cultured in media supplemented with blasticidin at 4 μg/mL (C6 and DU145) or 6 μg/mL (HCT116).

Library construction and selection of 5FC active clones. A bCD expression library encoding variants randomized across residues 149 to 159 was constructed, followed by insertion of randomized sequences spanning residues 310 to 320 (Supplementary Table S1). Six overlapping oligonucleotides (MB271-MB276) were used to synthesize a 256 bp DNA fragment including the 11 codons (149–159) that were randomized at 9% mutation frequency. The codons for the 310 to 320 residues were also randomized at 9%, and the 238 bp DNA fragment was synthesized using the six oligonucleotides, MB384-MB387, and MB267-MB268. Plasmid DNA purified from the 149 to 159 mutagenesis selection and the randomized 310 to 320 region fragment were digested with complementary restriction enzymes and ligated together. Transformation and selection for 5FC active mutants were performed as described previously using lower 5FC concentrations (10–0.5 μg/mL) in plate assays (14, 15).

Enzyme assays. The activity of wild-type and variant bCD lysates was assayed by monitoring the absorbance change due to the consumption of cytosine at 286 nm and the production of 5FU at 316 nm using an HP8452A Diode Array Spectrophotometer (Olis) at room temperature for 10 min following a protocol adapted from Hayden and colleagues (18). Cleared cell lysates were prepared as described previously (14). Selected bCDs were expressed in *E. coli* BL21 (DE3), and enzymes were purified by Ni-NTA chromatography and quantified as described (14). The kinetic constants were determined by plotting initial reaction rates fitted to the Michaelis-Menten equation using KaleidaGraph software (Synergy Software).

Construction of mammalian expression vectors. The wild-type and mutant *cod*A (encodes bCD) were subcloned as *Nco*I (blunt-ended)/*Xho*I fragments into pCDNA6/*myc*-HisB (Invitrogen) digested with *Eco*RV and *Xho*I. Site-directed mutagenesis was performed to overlay D314S mutation into pCDNA:1525 using QuikChange mutagenesis according to the manufacturer's protocol (Stratagene).

***In vitro* cytotoxicity assays.** One microgram of each plasmid DNA was used to transfect 1×10^5 C6, HCT116, and DU145 cells by lipofection using FuGENE 6 transfection reagent (Roche) at a 3:1 ratio according to the manufacturer's instructions. Protein expression level was determined by immunoblot analysis as previously described (19). For *in vitro* cytotoxicity assays, pools of transfectants were transferred to 96-well microtiter plates at an initial density of 500 (C6) or 1,000 cells per well (HCT116/DU145). After cell adherence overnight, 5FC (0–30 mmol/L) was added and the cells were incubated for 6 d, at which time the redox indicator dye Alamar Blue was added. Cell survival was determined by fluorescence recorded at a 530/590 nm as described by the manufacturer and data were plotted with the SD. At least three replicates were performed.

***In vitro* bystander effect assays.** C6, HCT116, and DU145 cells stably transfected with pCDNA were mixed at different ratios with stable transfectants harboring either pCDNA:bCD, pCDNA:1246, pCDNA:1525, or pCDNA:1779. The mixed cells were transferred to 96-well microtiter plates at final density as described above. After cell adherence overnight, 5FC [4 mmol/L (C6) or 10 mmol/L (HCT116/DU145)] was added and the cells were incubated for 6 d. Cell viability was determined as described above. At least three replicates were performed.

High performance liquid chromatography 5FC metabolite analysis. Stably transfected cells (HCT116) were plated in 6-well dishes (Corning) at a concentration of 4×10^4 cells per well. The reaction was stopped at various hours postdose (2.5 mmol/L 5FC) by adding 200 μL per well of 94:6 (v/v) acetonitrile/glacial acetic acid and the level of 5FU in cell lysates was

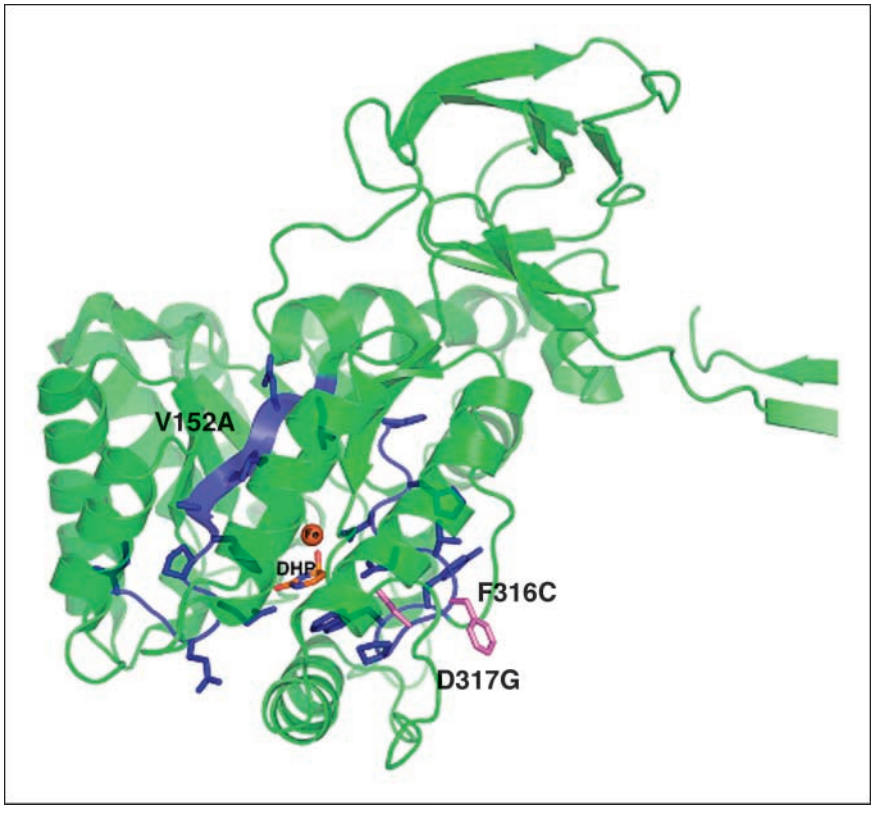

Figure 1. Cartoon diagram of wild-type bCD monomer. The 22 residues that were subjected to randomization and selection for 5FC sensitization are shown (*blue*). The location and identity of mutations (*V152A, F316C*, and *D317G*; 1525) that gave rise to highest specificity and activity toward 5FC are labeled in pink.

Table 1. Enzyme kinetics

	WT-bCD		1246		1525		1779	
	Cytosine	5FC	Cytosine	5FC	Cytosine	5FC	Cytosine	5FC
K_m (mmol/L)	0.46 (0.05)*	3.76 (0.4)	1.65 (0.34)	6.73 (2.07)	4.9 (1.11)	12.69 (4.53)	3.16 (1.8)	7.55 (0.84)
k_{cat} (sec^{-1})	49.68 (2.14)	19.71 (0.74)	2.13 (0.26)	83.68 (12.16)	1.69 (0.45)	101.74 (21.72)	2.98 (0.72)	115.24 (6.28)
k_{cat}/K_m ($mM^{-1}sec^{-1}$)	106.85 (39.3)	5.24 (1.87)	1.29 (0.76)	12.44 (5.88)	0.35 (0.4)	8.02 (4.8)	0.94 (0.46)	15.27 (7.47)
Relative efficiency to the wild-type	1	1	0.01	2.37	0.003	1.53	0.009	2.91
Relative substrate specificity †	0.95	0.05	0.09	0.91	0.04	0.96	0.06	0.94
Relative substrate specificity to the wild-type	1	1	0.09	18.2	0.04	19.2	0.06	18.8

Abbreviation: WT-bCD, wild-type bCD.
*Standard error.
†Cytosine: $[K_{cat}/K_m(\text{cytosine})]$ / $[K_{cat}/K_m(\text{cytosine})]$ + $[K_{cat}/K_m(5FC)]$; 5FC: $[K_{cat}/K_m(5FC)]/[K_{cat}/K_m(\text{cytosine})]$ + $[K_{cat}/K_m(5FC)]$.

detected using an isocratic, reverse-phase high performance liquid chromatography method.[4] Metabolite separation was carried out on a Phenomenex Luna C18 (2) analytic column (250 mm × 4.6 mm, 5 μm particle size) at a flow rate of 1 mL/min. The mobile phase was formic acid and water (1:99, v/v). 5FU was detected at an UV wavelength of 285 nm and eluted at 5.8 min. Total metabolite levels were calculated relative to a known concentration of an internal standard (5-chlorouracil).

Introduction of individual mutations at residues 316 and 317. The QuikChange kit was used to create amino acid substitutions F316C (MB480-481), F316L (MB482-MB483), F316V (MB484-MB485), D317G (MB478-MB479) F316C/D317G (MB490-MB491), F316L/D317G (MB492-MB493), and F316V/D317G (MB494-MB495). After DNA sequence confirmation, the resulting plasmids were designated pETHT:F316C, pETHT:F316L, pETHT:F316V, pETHT:D317G, pETHT:F316C/D317G, pETHT:F316L/D317G, and pETHT:F316V/D317G.

Xenograft tumor model. Pools of HCT116 cells stably transfected with pCDNA, pCDNA:bCD, or pCDNA:1525 [0.5×10^6 cells in 200 μL of PBS (pH 7.2)] were injected s.c. into the flanks of 5 to 6-wk-old female nude mice (n = 5; BALB/cAnNCr-nu/nu; National Cancer Institute). When tumors reached 3 to 4 mm (day 0), PBS or 5FC (375 mg/kg) was administered by i.p. injection twice a day for 21 d. Starting at day 0, the tumor volume was monitored using caliper measurement every other day, calculated using the formula: $4/3\pi$ [(width × length × height)/2] and analyzed for statistical significance using Student's t test.

X-ray crystallography. Three sequential mutations (V152A, F316C, and D317G) were introduced by site-directed mutagenesis into the wild-type bCD. The expression and purification of the resulting construct (1525) was carried out as previously described (20). Crystals of 1525 were grown in sitting drops by vapor phase equilibration against reservoirs containing 10% to 15% polyethylene glycol 6K, 200 mmol/L $MgCl_2$, and 100 mmol/L HEPES (pH 7–8). Crystals were grown using microseeds of wild-type enzyme crystals (transferred by streaking drops with a fiber) and grew within 1 wk to ~500 μm in each dimension. Crystals were cryo-preserved as previously described and found to be isomorphous with crystals of wild-type enzyme (16). Data were collected on a Rigaku RAXIS IV^{++} area detector, using X-rays produced by a Rigaku MicroMax-007 HighFlux (HF) microfocus X-ray generator (λ = 1.54Å). Data collection and reduction were performed using the CrystalClear software package (Rigaku). The structures were refined using the CCP4 crystallographic software suite (21).

Results and Discussion

Many factors limit the overall efficacy of current SGT approaches for cancer when CD and 5-FC are used. These include rapid turnover and clearance of 5FC in serum, inefficient gene delivery such that only a small population of tumor cells expresses the suicide gene, and poor enzyme activity toward the prodrug coupled with efficient competition for the enzyme's active site by the cells' endogenous pool of cytosine (1, 22–24). As a means to overcome these obstacles, we sought to create novel CD variants with significantly improved kinetic preferences toward 5FC. We used random mutagenesis to introduce multiple amino acid substitutions in two regions lining the active site of bCD and used both positive and negative selection in *E. coli* to identify variants with the ability to confer enhanced 5FC sensitivity to three cancer cell lines *in vitro* and *in vivo*. A similar strategy was used to identify several Herpes Simplex Virus thymidine kinase mutants with enhanced tumor ablation capabilities (25, 26). One such variant, SR39, is currently being used in a phase III clinical trial for prostate cancer. Although Herpes Simplex Virus thymidine kinase is widely used, there are two key reasons for optimizing additional suicide genes: (*a*) not all cancers are equally responsive to the same drug and (*b*) should treatment with one suicide gene fail, alternate suicide genes that the immune system has not been exposed to previously, could be used in additional rounds of therapy to ablate tumors.

Construction of random library and mutant selection. Previous studies revealed that individual point mutations in the substrate binding pocket of bCD, which confer sensitivity to *E. coli* at 1 μg/mL 5FC, do not achieve substantial *in vitro* activity. We therefore aimed to direct the bCD variants to evolve more efficiently toward 5FC by heavily randomizing the two regions lining the active site in a stepwise approach (Fig. 1). A single-targeted library randomized at the 149 to 159 residue region was initially generated and ~590 *E. coli* that harbored functional CD

[4] K. Serve, J.A. Yanez, C.M. Remsberg, N.M. Davies, M.E. Black. Development and validation of a rapid and sensitive HPLC method for detection of 5FC and its metabolites, submitted.

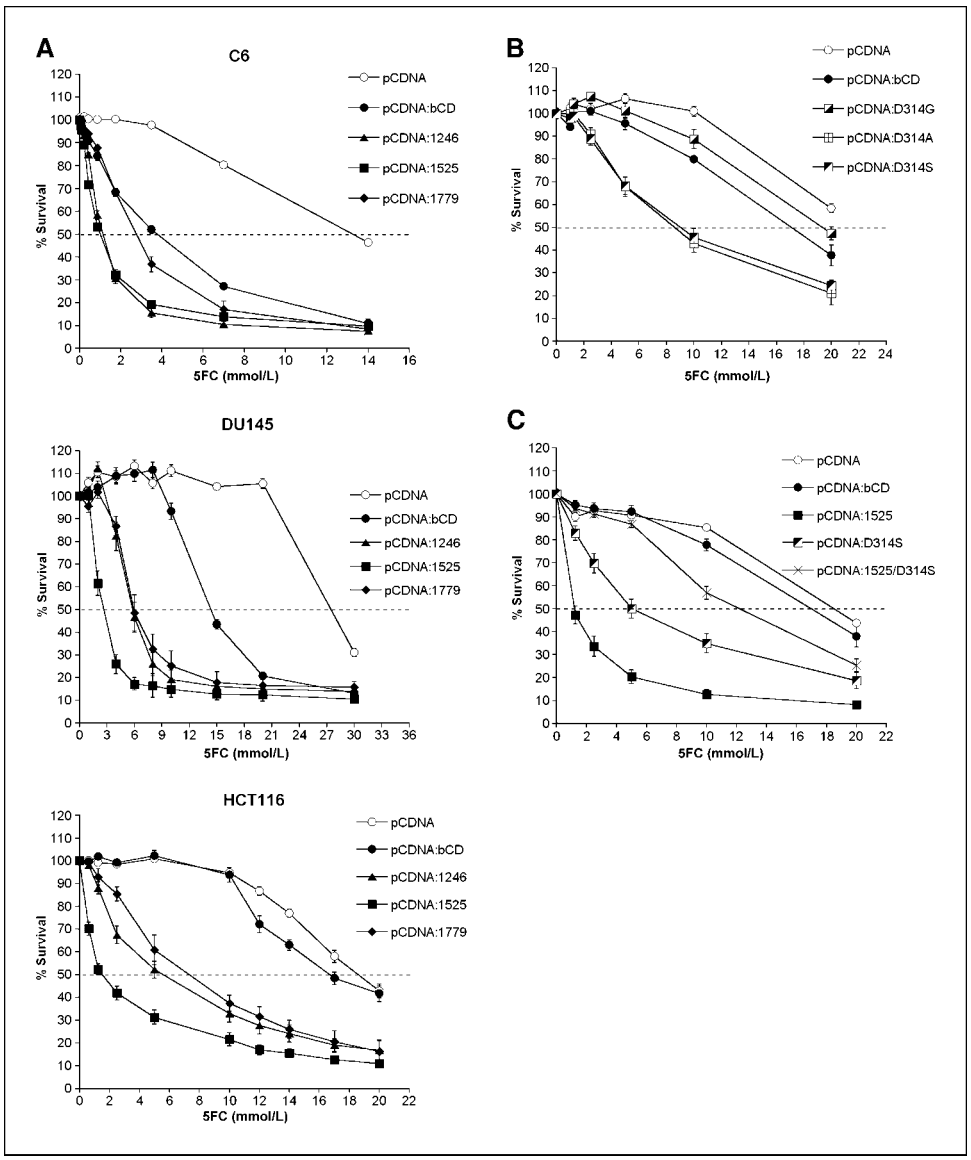

Figure 2. 5FC sensitivity assays of cells stably transfected with wild-type or mutant bCDs. Pools of stably transfected (*A*) C6, DU145, and HCT116 cells containing pCDNA, pCDNA:bCD, pCDNA:1246, pCDNA:1525, and pCDNA:1779 were evaluated for 5FC sensitivity. Pools of stably transfected HCT116 cells containing pCDNA, pCDNA:bCD, and (*B*) pCDNA:D314G, pCDNA:D314A, and pCDNA:D314S or (*C*) pCDNA:1525, pCDNA:D314S, and pCDNA:1525/D314S were evaluated for 5FC sensitivity. After 6 d of 5FC treatment, cell survival was determined using Alamar Blue according to the manufacturer's instructions. Each data point [*points,* mean (n = 3) of experiments performed with 24 replicates; *bars,* SE] is expressed as a percentage of the value for control wells with no 5FC treatment. Student's t test analysis determined that the differences in IC_{50} values between mutant bCD– and wild-type bCD–transfectants are statistically significant ($P \leq 0.05$).

were pooled. A second randomized coding region, corresponding to the incorporation of mutations across residues 310 to 320, was then introduced and ~3,700 enzymatically active variants were identified from an estimated 1.35×10^6 total number of transformants. Of those, 849, 365, 62, 20, and 12 clones conferred sensitivity at 20, 10, 2, 1, and 0.5 μg/mL 5FC, respectively. This lowest 5FC dose is 40-fold lower than the sublethal dose for *E. coli* expressing wild-type bCD.

Sequence analysis. Sequences of 47 variants sampled from each round of screening (data not shown) revealed that all targeted codons had at least one amino acid substitution. The average number of substitutions was 2.6, close to the theoretical average number of 2.1 for 9% randomization. Sequences of the 12 variants identified at 0.5 μg/mL 5FC were somewhat unexpected (Supplementary Table S2) because substitutions in the 149 to 159 residue region occurred infrequently and seemed unrelated to the degree of 5FC activity, and many of the same substitutions were observed in mutants with less or no 5FC activity. In contrast, the substitutions at the 310 to 320 residue region showed a strong relationship with 5FC sensitivity: in particular, substitutions at positions D317 and F316 with smaller hydrophobic residues were observed for the most active constructs. Few substitutions were observed at F310, G311, P318, W319, and Y320, suggesting these sites are important for overall catalytic activity or for structural stabilization. Sequence analysis reveals that the most active 12 mutants all have substitutions at D314, F316, and/or D317. As described in detail below, three mutants (called constructs 1246, 1525, and 1779) were identified as conferring sensitivity at significantly lower concentrations of 5FC, and were chosen for further characterization.

To elucidate the participation of individual amino acid substitutions at F316 and D317 found in all three constructs (1246, D314E/F316L/D317G; 1525, V152A/F316C/D317G; 1779, V315L/F316V/D317G), site-directed mutagenesis was used to generate the substitutions: F316L, F316C, F316V, D317G, F316L/D317G, F316C/D317G, and F316V/D317G. Results from *E. coli* complementation assays indicate that all mutants display CD activity, and that the individual D317G substitution and the double F316C/D317G substitutions found in 1525 seems to be

responsible for conferring the greatest degree of sensitivity to 5FC.

Enzyme assays of select mutants. To further characterize the 12 mutants identified by growth inhibition on plates containing 0.5 μg/mL 5FC, cell lysates were used initially to assess cytosine and 5FC conversion levels. Lysates of the mutants 1246, 1525, and 1779 showed the largest 5FC conversions of the variants and the wild-type, whereas the other variants displayed weak or no activity (data not shown). These three mutants and wild-type bCD were then purified to near homogeneity using a Ni-NTA chromatography column and their kinetic constants for cytosine and 5FC conversion were determined. All three random mutants display reduced kinetic parameters toward cytosine (Table 1). Mutant K_m values are increased 3.7- to 10.7-fold relative to wild-type bCD and k_{cat} values for the mutants range from 16.6- to 29-fold lower, corresponding to a 82.2- to 305.4-fold reduction in catalytic efficiency (k_{cat}/K_m). When 5FC is used as the substrate, K_m values are modestly increased 1.8 to 3.3-fold and k_{cat} values are increased 4.3- to 5.9-fold, to yield an overall improvement in k_{cat}/K_m for 5FC of 1.5- to 2.9-fold compared with wild-type bCD. The combination of reduced activity toward cytosine, and increased k_{cat} for 5FC, results in a significant (18.2- to 19.2-fold) shift in the relative substrate specificity toward 5FC relative to wild-type bCD.

***In vitro* analysis of mutant bCDs.** Mutant and wild-type *cod*A genes were cloned into the expression vector, pCDNA, and used to stably transfect C6, HCT116, and DU145 cell lines. Results from prodrug sensitivity assays show that all three variant bCD constructs confer increased sensitivity to 5FC, albeit to varying

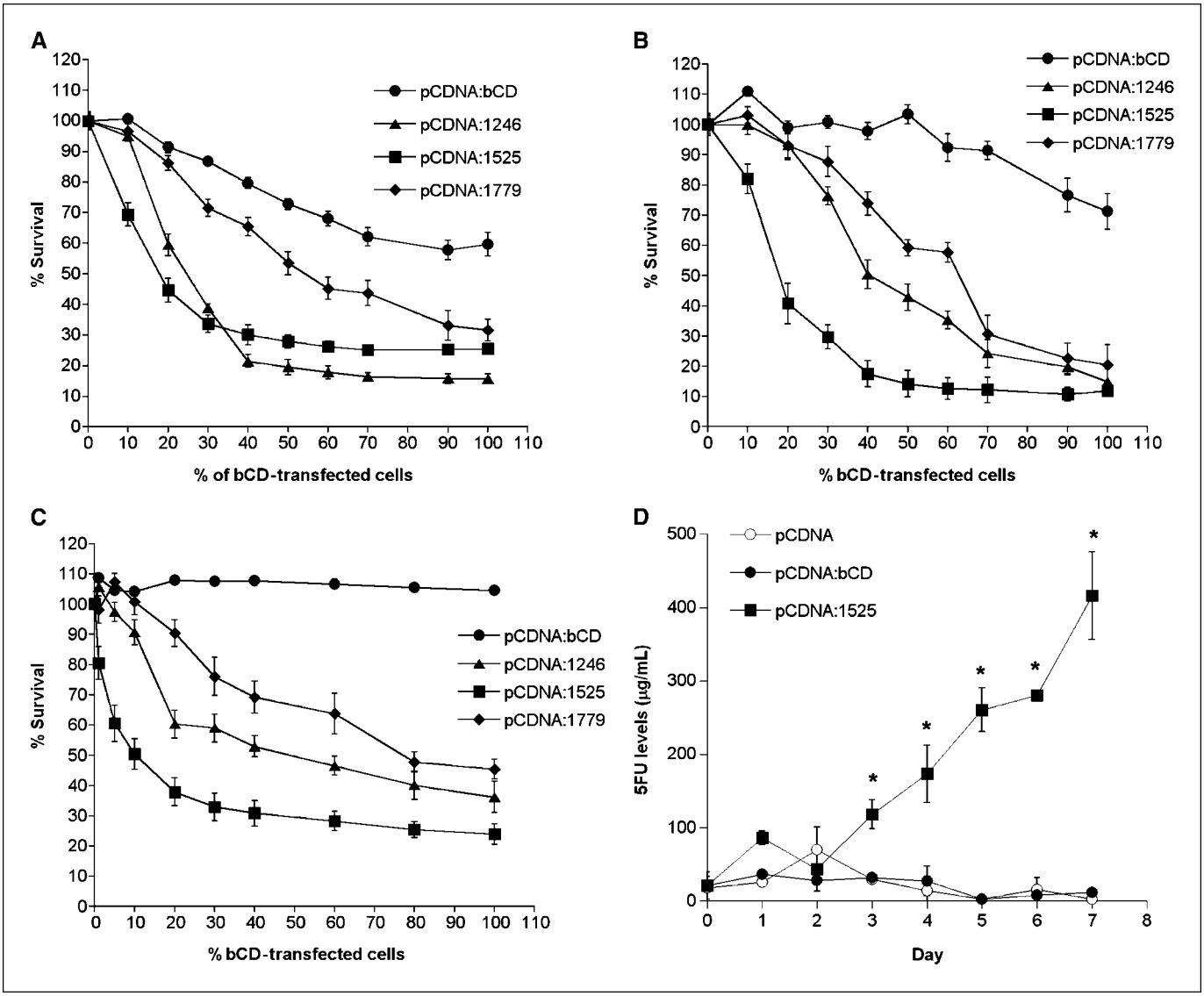

Figure 3. Bystander analysis of stable transfectants exposed to 5FC. Pools of (*A*) C6, (*B*) DU145, (*C*) HCT116 cells containing pCDNA were mixed with cells harboring either pCDNA:bCD, pCDNA:1246, pCDNA:1525, or pCDNA:1779 at different ratios and were subjected to 4 mmol/L (C6) or 10 mmol/L (DU145 and HCT116) 5FC for a period of 6 d, and cell survival was determined using Alamar Blue. Each data point [*points,* mean (n = 3) of experiments performed with 24 replicates; *bars,* SE] is expressed as a percentage of the value for control wells with vector-transfected cells. Student's t test analysis determined that the differences between percentage of mutant bCD– and wild-type bCD–transfectants needed to achieve 50% tumor cell killing are statistically significant ($P \leq 0.05$). *D,* high performance liquid chromatography analysis of 5FU levels in transfected cells. Stably transfected HCT116 cells were incubated with 2.5 mmol/L 5FC for up to 7 d and metabolite levels calculated relative to a known concentration of an internal standard. Student's t test was done to compare 1525 versus wild-type bCD–transfected cell lysates. *, $P \leq 0.005$ (days 3–4) and $P \leq 0.0003$ (days 5–7).

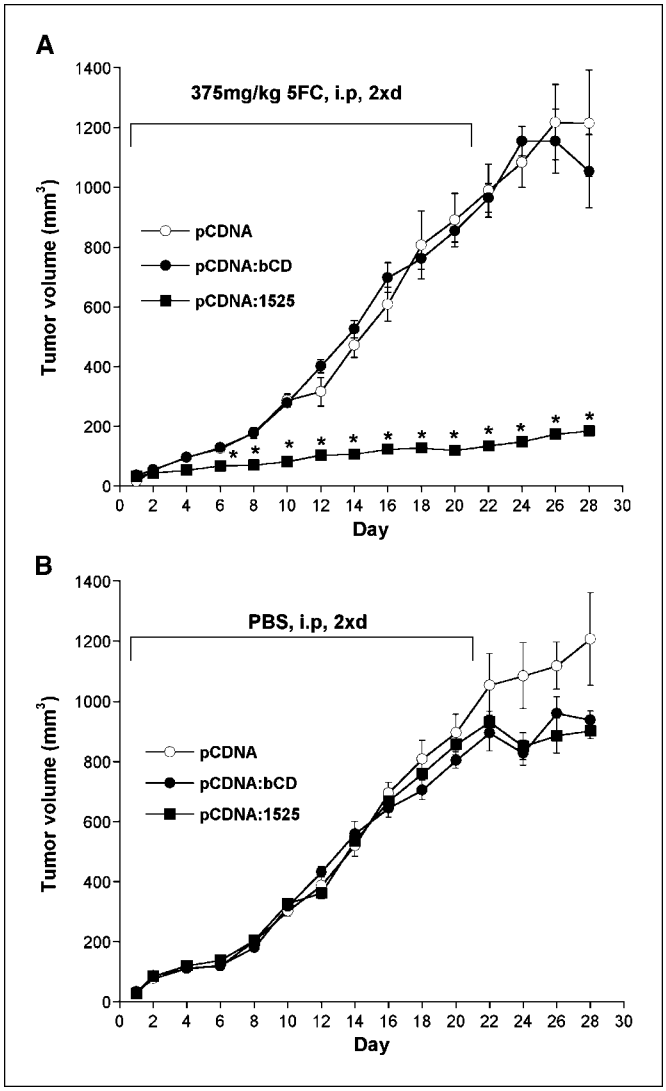

Figure 4. Tumor growth during and after 5FC treatment in a xenograft model. Pools of HCT116 cells transfected with pCDNA, pCDNA:bCD, or pCDNA:1525 were used to seed tumors in nude mice ($n = 5$). When tumor size reached 3 to 4 mm (day 0), (*A*) 5FC (375 mg/kg) or (*B*) PBS was i.p. administered twice a day for 21 d. Tumor growth was measured every other day for the duration of the experiment. Tumor volume was calculated using the formula $4/3\pi$ [(width × length × height)/2], plotted and analyzed for statistical significance using Student's *t* test. *, statistical significance ($P \leq 0.05$) in tumor sizes between mice harboring 1525-expressing tumor cells and those that received either empty vector– or wild-type bCD–expressing tumor cells in the presence of 375 mg/kg 5FC.

degrees in the different cell lines (Fig. 2*A*). In C6 transfectants, only a modest reduction in IC_{50} was observed compared with wild-type bCD–transfected cells (1.3- to 2.7-fold). The IC_{50} values of mutant bCD-transfected DU145 cells were 2.1- to 5-fold lower than wild-type bCD–transfectants. The mutants displayed the greatest reduction in IC_{50} values in HCT116 transfectants at 2.4 to 17-fold lower values than bCD. In all cell lines examined, 1525 consistently displayed the lowest IC_{50} values of the three mutants with the best response observed in HCT116 cells. We observed some cell line variance in the degree of 5FC sensitivity. Clinical studies indicate 5FU is an effective chemotherapeutic agent for colorectal, pancreatic, and breast cancer but is less effective for other types of cancers (27). Therefore, the observed cell line differences may simply be a reflection of inherent variations in drug sensitivity exhibited by individual cell types. Previously, we reported the construction and characterization of single site mutations at residue 314 (D314; ref. 14). Here, we sought to compare these D314 variants (D314G, D314A, and D314S) to the randomly derived mutants (1246, 1525, and 1779) and to explore the possibility that combinations of the best mutants from both series would yield an additive effect. Initially D314G, D314A, and D314S and wild-type bCD–transfected HCT116 cells were evaluated for 5FC sensitivity (Fig. 2*B*). Of the three D314 substitutions, D314S displays the greatest response to 5FC with an IC_{50} ~3.4-fold lower than that of wild-type bCD and ~5-fold higher than 1525-transfected cells. To assess the effect of the combination mutant, cells transfected with pCDNA, pCDNA:bCD, pCDNA:1525, pCDNA:D314S, and pCDNA:1525/D314S were subjected to *in vitro* 5FC sensitivity assays as described above. Results from this comparison indicate that the 1525/D314S overlay does not yield an increase in 5FC sensitivity over 1525 or the individual D314S mutant or wild-type bCD–transfected cells (Fig. 2*C*). Thus, the mutational routes toward optimal 5FC activation, generated by site-directed or randomizing mutagenesis, yield mutually exclusive sets of mutations that do not act synergistically. Below, we provide a possible explanation for this lack of additive response based on details that emerged from 1525 structure determinations.

Bystander effect. The three key mutants were further characterized for their ability to influence the killing of non-bCD–expressing cells through the bystander effect. Towards that end, populations of vector and bCD-transfected cells were mixed at various ratios and subjected to either 4 mmol/L (C6) or 10 mmol/L (HCT116 and DU145) 5FC for 6 days. The percentage of bCD-expressing cells needed to achieve 50% cell killing ranges from 20% to 50%, 20% to 60%, and 10% to 80% for C6, DU145, and HCT116 cells, respectively, when mutant bCDs were examined (Fig. 3*A–C*). In contrast, mixed populations containing wild-type bCD–transfectants displayed no cell killing effect in HCT116 cells and slight to modest effects in DU145 and C6 cells, respectively, and were unable to achieve 50% cell killing in any of the cell lines tested. Mutant 1525 displayed the greatest bystander effect in every cell line examined. In HCT116 cells this is most evident; when only 10% of 1525-expressing cells are present, 50% of the population is killed at a 5FC concentration at which 100% wild-type bCD population remains fully viable.

High performance liquid chromatography analysis of 5FU metabolites. Low transfection efficiencies in SGT impose a reliance on a robust bystander effect for tumor ablation. Although results from our kinetic studies suggest an improvement in 5FC deamination activity, we sought to more directly assess the production of 5FU by bCD-transfected cells by high performance liquid chromatography. Starting on day 3, the level of 5FU begins to accumulate in lysates from 1525-transfected cells and continues to increase from ~100 μg/mL at day 3 to ~400 μg/mL on day 7 (last time point) and reflects a 35.8-fold difference in 5FU levels between 1525 and wild-type bCD (Fig. 3*D*). This is in contrast to vector and bCD-transfected cell lysates that show no significant change in 5FU levels over the time course. Bystander experiments with 5FC revealed that all three variant bCDs showed a more robust cell killing in all three transfected cell lines compared with wild-type bCD–transfected cells. We suggest this is a direct reflection of the amount of 5FU produced in the transfected cells.

***In vivo* xenograft tumor model.** Mutant 1525 shows the best cell killing and bystander effect *in vitro* and was selected for further

analysis in an *in vivo* xenograft tumor model for human colorectal cancer. Tumor growth in all groups treated with PBS was indistinguishable with the exception of later points (Fig. 4). This statistically insignificant difference in the tumor volume near the end of the time course is likely due to the amorphous nature of the large tumors that made it difficult to obtain consistent measurements. Although no difference in tumor volume was observed between mice bearing vector or wild-type bCD tumors throughout or after the 5FC treatment period, the lack of significant tumor growth observed in mice bearing 1525 tumors is in stark contrast. From the time 5FC administration began to the maximum size, wild-type bCD tumors increased in volume from 34.4 to 1154 mm^3 (30.8-fold), whereas the 1525 tumors increased only from 32.5 mm^3 to maximum of 185 mm^3 (5.7-fold). Other studies using wild-type bCD show a reduced tumor growth rate using comparable doses of 5FC (28–30). In our hands, no significant antitumor response with wild-type bCD is observed at 375 mg/kg twice a day, whereas this dose provides a substantial growth restriction in 1525-bearing tumors. As such, 1525 provides significant improvement in tumor growth inhibition using a 5FC dose at which wild-type bCD tumors is completely unresponsive to.

Crystallographic analysis of bCD 1525. Crystals containing the enzyme in complex with the mechanism-based inhibitors 4-(R)-hydroxyl-3,4-dihydropyrimidine (DHP) or 5-fluoro-4-(S)-hydroxyl-3,4-dihydropyrimidine (5F-DHP) were generated out by soaking crystals in buffer containing 10 mmol/L 2-hydroxypyrimidine or 5-fluoro-2-hydroxypyrimidine (Aldrich), respectively. In these experiments, the pyrimidine compounds are converted enzymatically to a tightly bound hydrated adduct that mimics the enzyme transition state. The statistics for data collection and refinement are summarized in Supplementary Table S3.

Unbiased Fourier difference (F_{obs}-F_{calc}) maps were calculated using diffraction data of 1525 soaked in DHP and 5F-DHP (Fig. 5*A*), respectively, using the phase information calculated from a protein model consisting of the wild-type bCD enzyme (PDB accession code 1K70) with residues 152, 316, and 317 changed to alanine and the bound ligand DHP removed. The density of the bound compounds clearly showed the presence of bound compounds in positions nearly identical to those observed in the wild-type enzyme. The orientation of the pyrimidine ring within the density maps is confirmed by the presence of additional density in the 5F-DHP complex, corresponding to the additional fluorine substituent. However, compared with the wild-type enzyme, the compounds seem to exhibit significant conformational heterogeneity in the active site, particularly evident as disorder and minimal density at the C1 carbon position of both compounds. As a result, coordinates

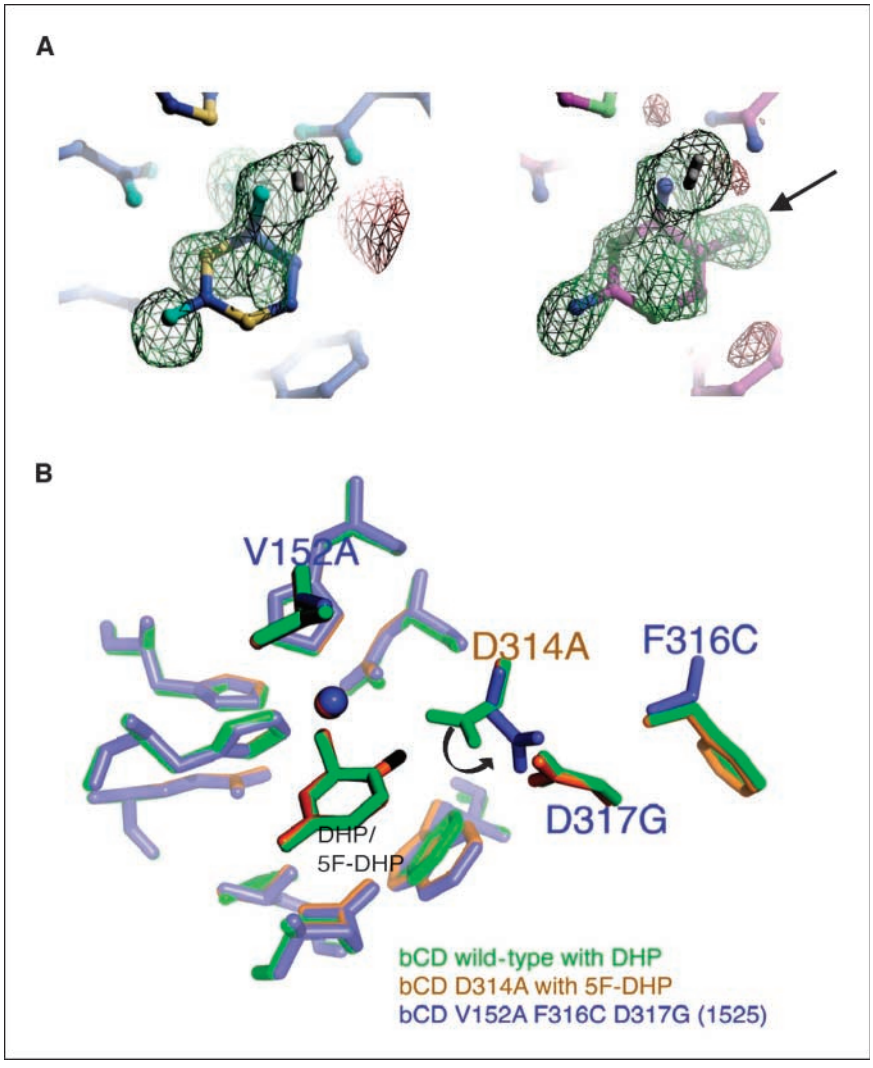

Figure 5. *A,* electron density for bound substrate analogue 2-hydroxypyrimidine (or DHP; *left*) and 5F-DHP (*right*) bound in the active site of bCD. As noted in the text, the density for the bound compound indicates disorder, particularly near the C1 carbon. However, the appearance of additional difference density corresponding to the 5-fluoro substituent (*arrow*) unambiguously confirms the orientation of the inhibitor. *B,* comparison of the active sites of wild-type and mutant bCD enzymes. Superposition of the active sites of wild-type bCD in complex with DHP (PDB accession code-1K70), D314A mutant in complex with 5F-DHP (PDB accession code-1RA5) versus 1525 soaked with 5F-DHP. The motion of residue D314 (*arrow*), into the cavity vacated by removal of a side chain in the D317G mutation, mimics the structural effect of the previously described D314A and D314G mutations.

of the bound compounds were not included in the final refined models of 1525. These structural models, along with the X-ray diffraction amplitudes, have been deposited in the RCSB structural database (accession code 3G77) to allow independent calculation of difference maps by interested investigators.

In the previously described structure of D314A mutant, the D314A substitution creates a hydrophobic pocket to accommodate the fluorine atom of 5F-DHP (16). This mutation not only eliminates a spatial clash with the fluorine atoms but also provides a favorable van der Waals contact with the bound 5F-DHP. In contrast, none of the three side chains mutated in the active site of 1525 are in direct contact with bound substrate. However, as a result of the mutation of D317 (which eliminates a carboxylate side chain), the wild-type residue D314, which is the side chain nearest to the 5′-position of the substrate, swings away from the active site (Fig. 5*B*), creating a neighboring cavity and reducing the local negative charge. This movement produces a similar chemical and structural effect as observed in D314A mutant.

Two other mutations (V152A and F316C) do not seem to affect the active site directly. This is further supported by experiments in which the substitutions found at F316 and D317 in 1246, 1525, and 1779 were individually examined for the ability to confer 5FC sensitivity in complementation assays. Close examination of the sequences at position D314 and D317 of the 12 bCD variants identified from the genetic complementation studies reveals D317G substitutions (but no D314A, S, or G substitutions) in nine of the isolates, whereas the remaining three clones have A or G substitutions at D314 but none at D317. Combining 1525 (V152A/F316C/D31G) and D314S substitutions resulted in a reversal of 5FC sensitivity rather than an additive effect. Taken together, these results support the notion that enhancement of 5FC activity occurs when mutations exist at D314 or the D317G substitution is present but that these substitutions are mutually exclusive.

Cancer chemotherapy treatments can result in significant and often debilitating side effects due to the absence of distinct biochemical differences that occur between normal and neoplastic cells. SGT provides an exceptional opportunity to introduce unique biochemical characteristics to cancer cells that can then be exploited for a safer, less toxic, and more effective treatment. Two suicide gene/prodrug systems have garnered significant attention and are undergoing preclinical and clinical evaluations; the widely used Herpes Simplex Virus thymidine kinase/ganciclovir and the CD/5FC systems (29). Despite initial enthusiasm for the use of these suicide gene/prodrug approaches, limitations such as insufficient gene delivery to the tumor site and poor prodrug conversion properties of the suicide enzymes have restricted the full potential of SGT. From over a million bCD mutants, we have identified one bCD variant (1525) that displays superior 5FC kinetic, cell killing, bystander, and tumor growth restriction activities. Collaborative studies using adenoviral vectors expressing mutant D314A in combination with radiotherapy to treat pancreatic cancer suggested that even the slight improvement of D314A provided enhancement of 5FC-mediated cytotoxicity *in vitro* and *in vivo* (31). Therefore, mutant 1525 will likely provide a significant advantage over wild-type bCD or D314A in at least three important ways: (*a*) by enhancing 5FC-mediated cell killing through both direct and bystander mechanisms; (*b*) by allowing the use of lower, less debilitating doses of 5FC to achieve effective cell killing; and (*c*) by providing an optimized alternative to the use of wild-type CD or Herpes Simplex Virus thymidine kinase SGT approaches. Furthermore, mutant 1525 may be used in a variety of different applications including for restenosis, noninvasive tumor imaging, and in negative selection systems.

Disclosure of Potential Conflicts of Interest

No potential conflicts of interest were disclosed.

Acknowledgments

Received 2/17/09; revised 3/18/09; accepted 3/20/09.

Grant support: NIH grants CA85939 (M.E. Black) and CA97328 (B.L. Stoddard and M.E. Black).

The costs of publication of this article were defrayed in part by the payment of page charges. This article must therefore be hereby marked *advertisement* in accordance with 18 U.S.C. Section 1734 solely to indicate this fact.

References

1. Nishiyama T, Kawamura Y, Kawamoto K, et al. Antineoplastic effects in rats of 5-fluorocytosine in combination with cytosine deaminase capsules. Cancer Res 1985;45:1753–61.
2. Katsuragi T, Sakai T, Tonomura K. Implantable enzyme capsules for cancer chemotherapy from bakers' yeast cytosine deaminase immobilized on epoxy-acrylic resin and urethane prepolymer. Appl Biochem Biotechnol 1987;16:61–9.
3. Springer CJ, Niculescu-Duvaz I. Gene-directed enzyme prodrug therapy (GDEPT): choice of prodrugs. Adv Drug Deliv Rev 1996;22:351–64.
4. Austin EA, Huber BE. A first step in the development of gene therapy for colorectal carcinoma: cloning, sequencing, and expression of *Escherichia coli* cytosine deaminase. Mol Pharmacol 1993;43:380–7.
5. Mullen CA, Kilstrup M, Blaese RM. Transfer of the bacterial gene for cytosine deaminase to mammalian cells confers lethal sensitivity to 5-fluorocytosine: a negative selection system. Proc Natl Acad Sci U S A 1992;89:33–7.
6. Dong Y, Wen P, Manome Y, et al. *In vivo* replication-deficient adenovirus vector-mediated transduction of the cytosine deaminase gene sensitizes glioma cells to 5-fluorocytosine. Hum Gene Ther 1996;7:713–20.
7. Huber BE, Austin EA, Richards CA, Davis ST, Good SS. Metabolism of 5-fluorocytosine to 5-fluorouracil in human colorectal tumor cells transduced with the cytosine deaminase gene: significant antitumor effects when only a small percentage of tumor cells express cytosine deaminase. Proc Natl Acad Sci U S A 1994;91:8302–06.
8. Mullen CA, Coale MM, Lowe R, Blaese RM. Tumors expressing the cytosine deaminase suicide gene can be eliminated *in vivo* with 5-fluorocytosine and induce protective immunity to wild type tumor. Cancer Res 1994;54:1503–06.
9. Haberkorn U, Oberdorfer F, Gebert J, et al. Monitoring gene therapy with cytosine deaminase: *in vitro* studies using tritiated-5-fluorocytosine. J Nucl Med 1996;37:87–94.
10. Lawrence TS, Rehemtulla A, Ng EY, Wilson M, Trosko JE, Stetson PL. Preferential cytotoxicity of cells transduced with cytosine deaminase compared to bystander cells after treatment with 5-fluorocytosine. Cancer Res 1998;58:2588–93.
11. Freeman SM, Abboud CN, Whartenby KA, et al. The "bystander effect": tumor regression when a fraction of the tumor mass is genetically modified. Cancer Res 1993;53:5274–83.
12. Moolten FL. Tumor sensitivity conferred by inserted herpes thymidine kinase genes: paradigm for a prospective cancer control strategy. Cancer Res 1986;46:5276–81.
13. Kuriyama E, Masui K, Sakamoto T, et al. Bystander effect caused by cytosine deaminase gene and 5-fluorocytosine *in vitro* is substantially mediated by generated 5-fluorouracil. Anticancer Res 1998;18:3399–406.
14. Mahan SD, Ireton GC, Stoddard BL, Black ME. Alanine-scanning mutagenesis reveals a cytosine deaminase mutant with altered substrate preference. Biochemistry 2004;43:8957–64.
15. Mahan SD, Ireton GC, Knoeber C, Stoddard BL, Black ME. Random mutagenesis and selection of *Escherichia coli* cytosine deaminase for cancer gene therapy. Protein Eng Des Sel 2004;17:625–33.
16. Ireton GC, McDermott G, Black ME, Stoddard BL. The structure of *Escherichia coli* cytosine deaminase. J Mol Biol 2002;315:687–97.
17. Ireton GC, Black ME, Stoddard BL. The 1.14 A crystal structure of yeast cytosine deaminase: evolution of nucleotide salvage enzymes and implications for genetic chemotherapy. Structure 2003;11:961–72.
18. Hayden MS, Linsley PS, Wallace AR, Marquardt H, Kerr DE. Cloning, overexpression, and purification of cytosine deaminase from *Saccharomyces cerevisiae*. Protein Expr Purif 1998;12:173–84.
19. Stolworty TS, Aaron MK, Candice LW, Ardiani A,

Cundiff J, Stoddard BL, Black ME. Yeast cytosine deaminase mutants with increased thermostability impart sensitivity to 5-fluorocytosine. J Mol Biol 2008; 377:854–69.
20. Ireton GC, Black ME, Stoddard B. Crystallization and preliminary X-ray analysis of bacterial cytosine deaminase. Acta Crystallogr D Biol Crystallogr 2001;57: 1643–5.
21. Collaborative Computational Project, Number 4. The CCP4 Suite: programs for protein crystallography. Acta Crystallogr D Biol Crystallogr 1994;50:760–3.
22. Trinh QT, Austin EA, Murray DM, Knick VC, Huber BE. Enzyme/prodrug gene therapy: comparison of cytosine deaminase/5-fluorocytosine versus thymidine kinase/ganciclovir enzyme/prodrug systems in a human colorectal carcinoma cell line. Cancer Res 1995;55: 4808–12.
23. Malet-Martino M, Jolimaitre P, Martino R. The prodrugs of 5-fluorouracil. Curr Med Chem Anti-Canc Agents 2002;2:267–310.
24. Kievit E, Bershad E, Ng E, et al. Superiority of yeast over bacterial cytosine deaminase for enzyme/prodrug gene therapy in colon cancer xenografts. Cancer Res 1999;59:1417–21.
25. Black ME, Newcomb TG, Wilson HM, Loeb LA. Creation of drug-specific herpes simplex virus type 1 thymidine kinase mutants for gene therapy. Proc Natl Acad Sci U S A 1996;93:3525–9.
26. Kokoris MS, Black ME. Characterization of herpes simplex virus type 1 thymidine kinase mutants engineered for improved ganciclovir or acyclovir activity. Protein Sci 2002;11:2267–72.
27. Harris BE, Manning BW, Federle TW, Diasio RB. Conversion of 5-fluorocytosine to 5-fluorouracil by human intestinal microflora. Antimicrob Agents Chemother 1986;29:44–8.
28. Kievit E, Nyati MK, Ng E, et al. Yeast cytosine deaminase improves radiosensitization and bystander effect by 5-fluorocytosine of human colorectal cancer xenografts. Cancer Res 2000;60:6649–55.
29. Greco O, Dachs G. Gene directed enzyme/prodrug therapy of cancer: historical appraisal and future prospective. J Cell Physiol 2001;187:22–36.
30. Niculescu-Duvaz I, Springer CJ. Gene-directed enzyme prodrug therapy: a review of enzyme/prodrug combinations. Expert Opin Investig Drugs 1997;6:685–703.
31. Kaliberova LN, Della Manna DL, Krendelchtchikova V, Black ME, Buchsbaum DJ, Kaleberov SA. Molecular chemotherapy of pancreatic cancer using novel mutant bacterial cytosine deaminase gene. Mol Cancer Ther 2008;7:2845–54.